Simple Method to Determine Linearity Deviations of Topography Measuring Instruments with a Large Range Axial Scanning System

Wilfried Bauer[a], Dorothee Hüser[b,*], David Gerbert[a]

[a] *Polytec GmbH, Polytec-Platz 1-7, 76337 Waldbronn, Germany*
[b] *Physikalisch-Technische Bundesanstalt, Bundesallee 100, 38116 Braunschweig, Germany*

Abstract

The use of areal characterization of surface texture with high accuracy in a quality control process requires reliability. Therefore, regular inspection of the measurement systems is needed. Important metrological features of a measurement system in dimensional metrology are the amplification factor and linearity.

This paper presents a simple method for characterizing the axial scanning system of areal topography measuring instruments with little expense and effort, well suited for industrial routine calibration in the field. The method is based on employing a single material measure with a range of step heights. It is shown that the amplification factor and linearity deviations can be determined and adjusted for large axial measurement ranges.

Keywords: surface topography, topography measurement, amplification factor, linearity, calibration, step height standards, uncertainty, large range axial scanning

1. Introduction

There is growing demand for quality assessment of the dimensional properties of work pieces that have both form and surface texture. In addition, in many cases areal measurements of surface topography (texture and form de-

*Corresponding author
Email address: dorothee.hueser@ptb.de (Dorothee Hüser)

viation) are required rather than simple line profiles, which may not provide enough information needed for characterizing the functional behavior of the surface. A variety of optical measuring instruments is available for areal topography measurement with high accuracy. The upcoming standard ISO 25178-700 [1] on calibration, adjustment and verification of areal topography measuring instruments meets requirements of increasing accuracy and traceability of areal measurement systems and include optical measuring instruments.

However, calibration of the instrument axial scanning system (z-axis) over large scan ranges may be time consuming. Some instruments provide scan ranges up to 70 mm in axial direction [2]. For large scan ranges of the z-axis small sized linearity deviations need to be determined along the complete range. In order to fulfill ISO 9001 [3] regulations, instrument calibration has to be carried out within defined time intervals. The purpose of such routine calibration in industry is to check, whether instruments are still working appropriately. The routine calibration procedure, therefore, needs to be fast, simple and able to be realized in the field by the regular staff. In this paper, a method that meets the requirements of being simple and easily performed in the field has been developed.

To obtain the *response curve* (in the international vocabulary of metrology VIM [4] referred to as *calibration curve*) of an axis typically requires costly setups with an interferometer or complex procedures employing material measures being positioned at many locations [5] within the measurement range or representing a number of steps [6]. The method of Kiyono et al. [5] shows that a response curve of the z-axis can be obtained if a relationship of the step heights, which are differences of positions rather than absolute positions, is maintained. Giusca and Geol have developed a measurement strategy employing a flat plane of optical precision with accurately adjusted tilt angles [7]. This method is suitable for instruments with a z-axis in the micrometer range.

To overcome the need of a more accurate external positioning stage and to be suitable for instruments with a range of the z-axis of several millimeters, Boedecker et al. [6] employ a material measure representing a number of steps.

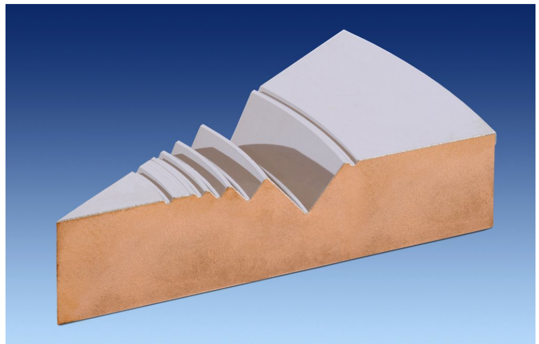

Figure 1: Material measure representing 6 different height resp. depth values, here with nominal depth values $d = 5, 50, 450, 100, 2000$, and $5000\,\mu$m. The nominal width at the bottom is $w = 300\,\mu$m and the nominal with between neighboring groove top edges is $400\,\mu$m delivering areas of widths of $100\,\mu$m and $200\,\mu$m for evaluation of the depths, see Fig. 7.

This is realized by a combination of material measures firstly representing coarse step heights covering the complete z range and secondly, fine step heights covering small sections of the range. The combination of the measurements on the object with the fine heights and those on the object with the coarse heights requires a time consuming calibration process and certificates for the material measures are often not available. In Leach et al. [8], a review is presented on procedures to measure metrological characteristics (MCs) with a variety of material measures each representing one or more specific MC. They show step height artefacts, one of the kind employed by Boedecker et al. [6], see Fig. 9 in [8], and the depth setting type used during the investigations of the present paper, see Fig. 8 in [8].

Guisca et al. [9] show linearity deviation studies that are performed by measuring four different height or depth values. Here, the amplification factor determination is based on the relationship between the calibrated height values and the measured height values, i.e. solely on the differential relationship of positions

$$d_{\mathrm{In}} \;=\; \alpha_{\mathrm{z}}\, d_{\mathrm{C}} \;+\; r \tag{1}$$

with α_{z} in ISO 25178-600 being called the *amplification factor*, if the quantity

d_{C} is the *actual input quantity* and d_{In} the *measured quantity*. In Guisca et al. [9], the values of quantity d_{C} represent the *calibrated values* of the material measure with uncertainties presumed to be significantly smaller than those of the *measured quantity*, in wording of VIM [4] the *indicated quantity* d_{In}, allowing the use of d_{C} as regressor of a linear regression problem. The wording for *values of 'measured' quantity* in ISO 25178-600 refers to the *'indicated' values* in VIM, while the wording 'calibrated values' used in Guisca et al. refers to 'measured quantity value' in VIM.

With the presumption that the input quantity of the calibrated values has negligible random effects and r are residuals due to random effects of the instruments indication that are normally distributed, the factor α_{z} is estimated by linear regression

$$\min_{\alpha_{\mathrm{z}}} \left\{ \sum_{i=1}^{n} r_i^2 \right\} \quad \text{with} \quad r_i \;=\; d_{\mathrm{In},i} \;-\; \alpha_{\mathrm{z}}\, d_{\mathrm{C},i} \tag{2}$$

and with $i = 1, \ldots, n$ pairs of measurement and calibration values of the heights or in case of depth setting artefacts, i.e. grooves, pairs of measurement and calibration values of the depths, yielding

$$\alpha_{\mathrm{z}} \;=\; \frac{\sum_{i=1}^{n} d_{\mathrm{In},i}\, d_{\mathrm{C},i}}{\sum_{i=1}^{n} d_{\mathrm{C},i}^2}. \tag{3}$$

The residuals of a regression of this relationship are an estimate of the uncertainty of the linearity. However, if systematic non-linear behavior dominates, the absolute position of the location of the step heights with respect to one common origin is required.

With this paper, we show that an estimate of linearity deviations can be carried out in the field. To overcome the lack of an absolute scale z_{C}, a 'ladder' is constructed of n_{p} 'flights' of n_{d} 'rungs', as illustrated in Fig. 2. The construction of the scale z_{C} is achieved by using a small number of steps or grooves on one artefact and with low cost positioning at a small number of locations along the range of the z-axis. In the case of depth setting artefacts (grooves), the 'ladders' are built downwards, starting with the top floor and successively going downward. If the distance between two successive floors fits the rung heights, as

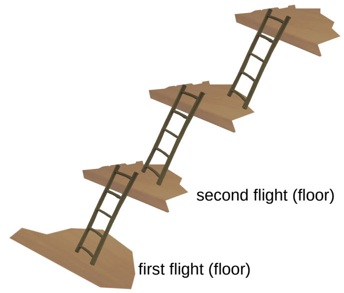

Figure 2: Illustration of the idea to construct an absolute scale by stitching measurements of different connected step heights (like rungs/ steps of one ladder) at successive positions (flights or floors). As the flights are connected by successively using the ladder.

illustrated in Fig. 2, then the true ladder length can be assembled from multiples of a previous measured length of a single ladder.

The idea of the measurement strategy is to stitch intervals covered by the steps of the material measure to characterize the z-axis of an instrument. The procedure is demonstrated using as example an areal coherence scanning interference measurement system with the z-axis being driven by an electro-magnetic actuator. Furthermore, the determination of the linearity deviation is verified with the aid of synthetically generated response curves with sinusoidal linearity deviation.

2. Measurement strategy

The German national metrology institute Physikalisch-Technische Bundesanstalt (PTB), for instance, provides material measures with five or six parallel grooves of varying depth in one object with the reference plane for all grooves being at the same level, see Fig. 1. This artefact ensures the grooves have a fixed relationship with respect to each other.

The material measure used for the investigations presented in this paper has the following nominal depth values d:

$$d/\mu\text{m}: \quad 5 \quad 50 \quad 450 \quad 1000 \quad 2000 \quad 5000$$

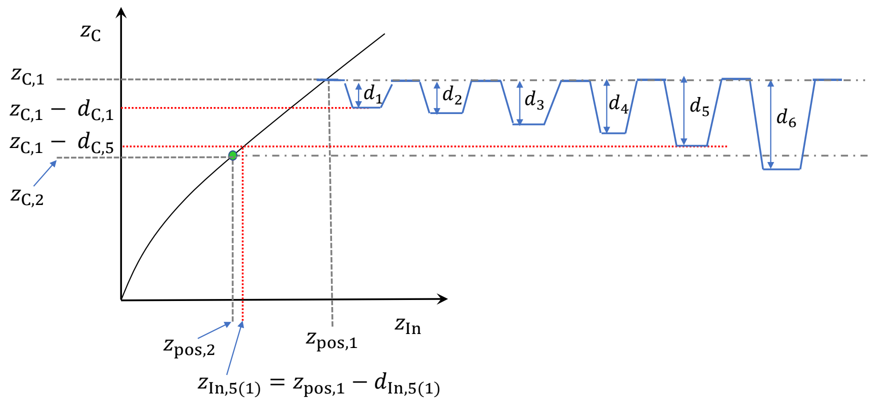

Figure 3: Principle of relating depth setting artefacts with the response curve of the z-axis of a topography measuring instrument. For each physical translation of the depth setting artefact $k = 1, \ldots, n_{\mathrm{p}}$ exist $j(k) = 1, \ldots, n_{\mathrm{d}}(k)$ different depth measurements, with $n_{\mathrm{d}}(k) \geq 6$. The plane of the position of the reference plane of the k-th physical translation of the material measure, here indicated by a dashed doted lines, is the value obtained by the measurement of the reference plane $z_{\mathrm{pos},k}$ here with $k = 1$ and $k = 2$.

The nominal groove width at the bottom is $w = 300\,\mu$m and the nominal width between neighboring grooves is $400\,\mu$m.

The material measure is measured at different positions along the axial scanning system (referred to as z-positions z_{pos}) along the measurement range with the distance between neighboring z-positions approximately being of the same size as the depth of the largest groove. Fig. 3 shows how the concept of stitching or assembling an absolute axis like constructing a 'ladder' from successive 'ladders' is applied to measurements with a PTB depth setting artefact. Since for the present material measure, each 'flight' of n_{d} 'rungs' has the same properties, the start of the 'ladder' can be set so that it is convenient for determining the non-linearities, provided this start position is recorded. The 'flights' will be denoted by the index k and the level of a 'rung' , complying with a step height or a groove depth d, by the index j. If a ladder connects a pair of 'flights' k and $k+1$ then the measured groove depth, analogous to the 'rung level' is labeled with the index $j(k)$ and denoted as $d_{\mathrm{In},j(k)}$.

For a measured groove $j = 5$ at physical translation position $k = 1$ the z-position of the bottom of groove as drawn in Fig. 3, the 'indicated' z-position of the groove bottom $z_{\mathrm{In},j(k)}$ is obtained by $z_{\mathrm{In},j(k)} = z_{\mathrm{pos},k} - d_{\mathrm{In},j(k)}$. Locating the depth setting artefact at different z-positions may, for example, be realized by using gage blocks or other plane parallel objects to mount it.

The absolute calibrated scale, the dependent quantity, of the response curve characterizing linearity deviations is uncertain mainly due to the lack of knowledge of an absolute start position, due to the ambiguities of presumptions on the interpolating model to assemble the 'ladder' and 'flights', and to the size of the steps (distance of 'rungs'). These uncertainty influences are dependent on the specifics of the depth setting artefact (choice of the 'rung' distances) and on the spatial wavelength of the linearity deviations of the instrument's z-axis. In Section 5, one example evaluating experimental data and estimating uncertainty influence factors by a Monte Carlo simulation is given.

The number of grooves is n_d (here it is $n_\mathrm{d} = 6$) and the number of positions in which the material measure is located is n_p, then $N = n_\mathrm{d} n_\mathrm{p}$ data points are obtained. For some positions repetitive measurements have been performed, so that the total number N is larger than $n_\mathrm{d} n_\mathrm{p}$. The PTB calibration certificate provides $j = 1, \ldots, n_\mathrm{d}$ depth values for each of the grooves referred to by $d_{\mathrm{C},j}$, the measurements deliver $k = 1, \ldots, n_\mathrm{p}$ values for the z-positions of the objects' reference plane location $z_{\mathrm{pos},k}$ and N different depth values $d_{\mathrm{In},j(k)}$. For simplicity, the index notation throughout this paper omits dealing with repetitive measurements.

3. Analysis method

The analysis method consists of two steps

1. Estimation of the adjusted, i.e. calibrated, positions $z_{\mathrm{C},k}$ of the object location due to the calibrated values of the material measure.
2. Estimation of the scaling or amplification factor and the linearity deviation curve.

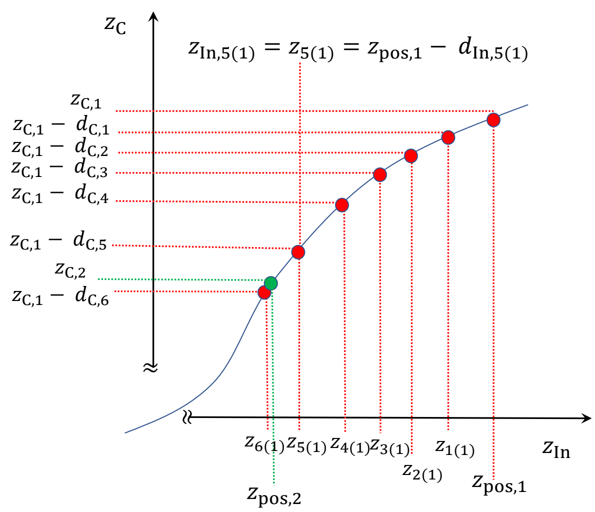

Figure 4: Illustration that a function $f_k\colon z \mapsto f_k(z)$ fitted to the measurements of the k-th ensemble of n_d (here it is $n_\mathrm{d} = 6$) grooves of one object delivers the reference position $z_{\mathrm{C},k+1}$ of the subsequent, the $k+1$-st position.

Step 1 is performed by deriving a value $z_{\mathrm{C},k+1}$ of the position with respect to the calibrated absolute axis from the depth measurements of all grooves performed at the previous location $z_{\mathrm{pos},k}$ and the measured position of the reference plane $z_{\mathrm{pos},k+1}$. To do this, the indirect quantity is the absolute reference scale z_C and the direct experimentally observed quantity, with its values referred to as indicated values, z_In.

In Step 1 a fit model function $f_k\colon z_\mathrm{In} \mapsto f_k(\mathbf{p}, z_\mathrm{In})$ of the response curve with model parameter vector $\mathbf{p}$ along the interval that is covered by the largest depth according to à priori knowledge is used. Here, a parabola with coefficient vector $\mathbf{p}_k$ has been chosen

$$f_k(z_\mathrm{In}) \;=\; \sum_{\nu=0}^{2} p_{k,\nu}\,\left(z_\mathrm{In} + \varepsilon_\mathrm{In}\right)^\nu + \varepsilon_\mathrm{C} \quad \text{with} \quad \mathbf{p}_k = (p_{k,0}, p_{k,1}, p_{k,2})^\mathsf{T} \qquad (4)$$

and with $(\varepsilon_\mathrm{In}, \varepsilon_\mathrm{C})$ being the deviation vector of data points perpendicular to the curve of the function f_k with estimated parameters $\mathbf{p}_k$. To simplify the implementation of the algorithm to estimate the model parameters by linear regression, only residuals ε_C are considered. This can be justified with regard to the fact that the complete model is an approximation that can only be used for linearity deviations of long spatial wavelengths. Future work is planned to compare various models including Bezier splines with total least-squares fits investigating the limitations of the procedure.

For all depth measurements carried out at the location with the position of reference plane $z_{\mathrm{pos},k}$, the observed positions of the groove bottoms respectively the top of step heights are evaluated by

$$z_{\mathrm{In},j(k)} = \begin{cases} z_{\mathrm{pos},k} & + & d_{\mathrm{In},j(k)} & \text{for step heights} \\ z_{\mathrm{pos},k} & - & d_{\mathrm{In},j(k)} & \text{for grooves.} \end{cases} \tag{5}$$

Furthermore, in the case of depth setting artefacts, the sequence of translation positions is chosen such that the highest is the first and in the case of step heights the lowest is the first. The first calibrated position $z_{\mathrm{C},1}$ is set to the measurement value of the first measured position $z_{\mathrm{pos},1}$. The calibration value $z_{\mathrm{C},k+1}$ of the successor of the physical translation with number $k+1$ is then obtained by inserting the corresponding measurment value of the translation of the reference plane on the object at $z_{\mathrm{pos},k+1}$ into the model function f_k of position k of the physical translation of the object with $k, k+1 \in \{1, \ldots, n_\mathrm{p}\}$.

$$z_{\mathrm{C},k+1} = f_k(z_{\mathrm{pos},k+1}). \tag{6}$$

The parameters $p_{k,\nu}$ of each model function f_k, here, for instance, the coefficients $p_{k,0}$, $p_{k,1}$, $p_{k,2}$ of the parabola, are obtained by fitting the target function to the set of $n_\mathrm{d}(k)$ points $(z_{\mathrm{C},k} - d_{\mathrm{C},j},\, z_{\mathrm{pos},k} - d_{\mathrm{In},j(k)})$ with $j(k) = 1, \ldots, n_\mathrm{d}(k)$ and with the target function

$$z_{\mathrm{C},k} - d_{\mathrm{C},j} = f_k(p_{k,\nu}, z_{\mathrm{pos},k} - d_{\mathrm{In},j(k)}) + r_{j(k)} \tag{7}$$

solving the optimization problem

$$\min_{p_{k,\nu} \forall \nu} \left\{ \sum_{j(k)} r_{j(k)}^2 \right\} \tag{8}$$

with ν being the index for the different model parameters and $p_{k,\nu}\ \forall\nu$ being the notation to search the minimum 'for all parameters $p_{k,0}, p_{k,1}, \ldots$'.

For the model example parabola, Eq. 4, the model parameters are the coefficents $p_{k,0}, p_{k,1}, p_{k,2}$ of the parabola $f_k(z_{\mathrm{In}}) = p_{k,2}\left(z_{\mathrm{pos},k} - d_{\mathrm{In},j(k)}\right)^2 + p_{k,1}\left(z_{\mathrm{pos},k} - d_{\mathrm{In},j(k)}\right) + p_{k,0}$ are varied until $\sum_{j(k)}\left(z_{\mathrm{C},k} - d_{\mathrm{C},j} - f_k\left(z_{\mathrm{pos},k} - d_{\mathrm{In},j(k)}\right)\right)^2$ reaches its minimum.

Fig. 3 and Fig. 4 illustrate the idea of sequentially fitting curves to the sets of $n_{\mathrm{d}} = 6$ or in case of repetitions of $n_{\mathrm{d}}(k) > 6$ points to obtain the response curve z_{In} vs. z_{C}.

Step 2: the estimation of the amplification factor α_{z} and the linearity deviation $r(z)$ is based on the model function

$$z_{\mathrm{In}} = \alpha_{\mathrm{z}}\, z_{\mathrm{C}} + z_0 + r(z_{\mathrm{C}}) \tag{9}$$

with α_{z} denoting the amplification factor, z_0 a constant offset and the function r denoting the residual non-linearity depending on the position z_{C}. In ISO 25178-600 [10], the maximum of the residuals is defined as *linearity deviation* of the z-axis

$$l_{\mathrm{z}} = \max\left\{r(z_{\mathrm{C}})\right\}. \tag{10}$$

The two parameters α_{z}, z_0 are obtained by linear regression fitting a straight line to all N points $(z_{\mathrm{pos},k} - d_{\mathrm{In},j(k)}, z_{\mathrm{C},k} - d_{\mathrm{C},j})$, i.e. using all $j(k) = 1, \ldots, n_{\mathrm{d}}(k)$ measurements for all $k = 1, \ldots, n_{\mathrm{p}}$.

4. Verification of the procedure

The procedure is verified using synthetic data with known linearity devation function r: $z \mapsto r(z)$. Here, sinusoidal linearity deviations of amplitudes $a_{\mathrm{d}} = 1\,\mu$m, $0.5\,\mu$m, and $1.5\,\mu$m and wavelengths $\lambda = 30$ mm and 70 mm along a measuring range of 35 mm have been generated

$$z_{\mathrm{In}} = \alpha_{\mathrm{z}}\, z_{\mathrm{true}} + a_{\mathrm{d}} \cos\left(\frac{2\pi}{\lambda}\left(z_{\mathrm{true}} + \Delta z\right)\right) \tag{11}$$

with α_{z} denoting the amplification factor, a_{d} the amplitude, λ the wavelength, and Δz the phase shift of the linearity deviation. Furthermore, as phase shift Δz

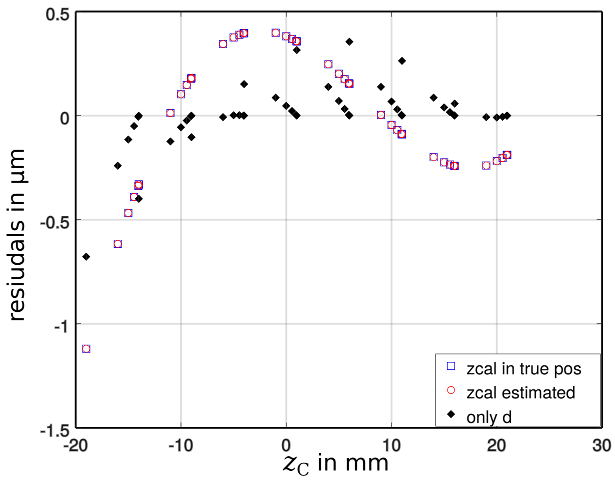

Figure 5: Simulation showing the linearity deviation as residuals of fitted regression lines, the blue squares obtained from instrumental values $z_{\mathrm{In},j(k)}$ as of Eq. (11) vs. true values and red circles vs. estimated values $z_{\mathrm{C},k} - d_{\mathrm{C},j}$. The black, filled diamonds are the residuals of a regression line fitted to $d_{\mathrm{In},j(k)}$ vs. $d_{\mathrm{C},j}$.

the values 0 and 10 mm have been chosen. The wavelengths are large compared to the measurement range so that parabolas are appropriate model functions $f(z_\mathrm{In}) = z_\mathrm{C}$ for intervals of 5 mm, which is the depth of the largest groove of the material measure.

Fig. 5 shows the residuals of the line fitted to all N pairs of data points $\left(z_{\mathrm{In},j(k)}, (z_{\mathrm{C},k} - d_{\mathrm{C},j})\right)$ as red circles, while the blue squares show the residuals of the regression line fitted to N pairs $\left(z_{\mathrm{In},j(k)}, z_{\mathrm{true},j(k)}\right)$. The parameters chosen to generate the simulated data set of Fig. 5 are $\lambda = 70\,\mathrm{mm}$, $\Delta z = 10\,\mathrm{mm}$, $a_\mathrm{d} = 1.5\,\mu\mathrm{m}$, and $\alpha_\mathrm{z} = 0.99990$.

The figure illustrates that simply evaluating the regression according to the depth values $d_{\mathrm{In},i}$ vs. $d_{\mathrm{C},i}$, which are displayed as black, filled diamonds, does not give a correct characterization of the linearity deviation of the instrument axis. The residuals obtained by our method of successive estimation of calibrated positions, however, deviate very little, less than $10^{-4}\,\mu\mathrm{m}$, from the synthetic residuals. The small finite deviation is mainly caused by the offset between the

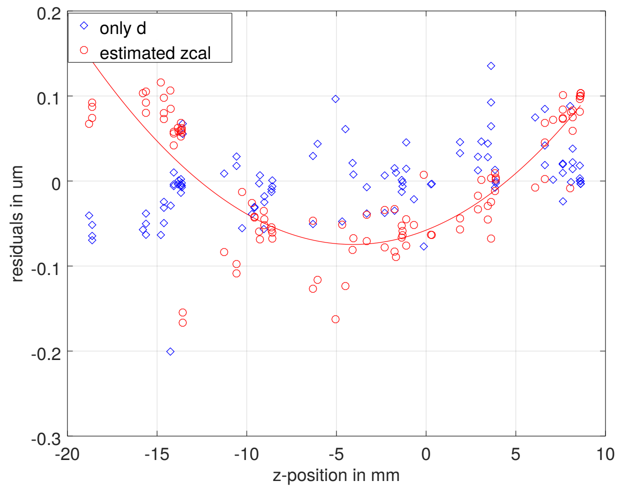

Figure 6: Measurement by a Polytec coherence scanning interferometer with blue diamond symbols showing the residuals of a regression line fitted to $d_{\mathrm{In},j(k)}$ vs. $d_{\mathrm{C},j}$ and red circles showing the result using absolute positions with estimated values $z_{\mathrm{C},k} - d_{\mathrm{C},j}$. The systematic trend of non-linearity visible for the red circles is emphasized by a parabola drawn as red curve.

first measured position with respect to the unknown true value. Furthermore, a contribution to the deviation is due to the uncertainty of the model functions f_k. Here, the uncertainty is due to the approximation of a segment of a cosine by a parabola.

5. Measurement results

The measurement example of Fig. 6 showing a result obtained by routine calibration of the instrument in the non-ideal field environment illustrates that the procedure presented here can reveal systematic effects of non-linearity. This would be unrecognizable if only the relationship between measured and calibrated values of the groove depths is regarded without any estimation of the absolute position within the range of the z-axis.

Two contributions to the uncertainty of the result have already been mentioned above: the ambiguity of the value for the first position $z_{\mathrm{C},1}$ and the

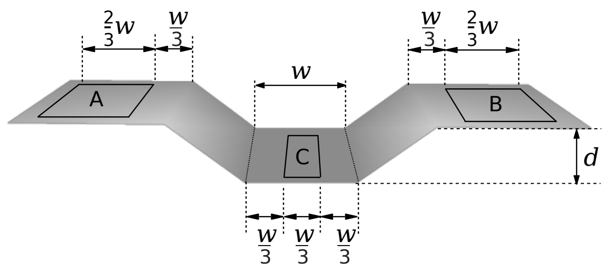

Figure 7: The depth of each groove is evaluated by fitting two parallel planes to data sets on the reference plane within regions A and B in the vicinity of the groove and within a region at the center of the groove bottom area C. The nominal width at the groove bottom of the artefact shown in Fig. 1 is $w = 300\,\mu$m and the nominal width between neighboring groove top edges is $400\,\mu$m, such that the two reference planes at the sides of one groove have a distance of $100\,\mu$m to the edges and a width of $200\,\mu$m. The plane of the bottom center has a width of $100\,\mu$m.

uncertainty of the model functions f_k. The latter has two components, first that the choice, here for instance the parabola, does not apply to the behavior of the instrument within each of the intervals sized the depth of the largest groove.

Secondly, the uncertainties $u(d_{\mathrm{C}})$ of the depth values given in the calibration certificate of the material measure as well as the uncertainties $u(d_{\mathrm{In}})$ of the depth values measured by the instrument under investigation are contributing.

Another contribution is the uncertainty of the whole artefact measurement is its tilt within the field of view, which is mainly influenced by the flatness deviation[1] of the reference surface. The flatness deviation results in a shift of the reference areas of the grooves with respect to each other. The tilt of the object, uncertainties of the lateral scales together with the coarseness of the depth of grooves contributes to ambiguities of linearity deviations of small spatial wavelength. The uncertainty contributions of the depth measurement uncertainties $u(d_{\mathrm{C}})$ and $u(d_{\mathrm{In}})$ together with the shifting of reference areas behave like wobbly

[1]orthogonal deviation of the reference surface from planarity

	$u(d_i)$	c	u_{r}
d_{C}	$0.1\,\mu$m	$0.5\ldots1$	$0.05\ldots0.1\,\mu$m
d_{In}	$0.3\,\mu$m	$0.4\ldots1$	$0.1..0.3\,\mu$m
d_{bow}	$0.3\,\mu$m	1.3	$0.38\,\mu$m

Table 1: Uncertainty contributions of the influencing components with uncertainties given in column 2, the sensitivities of the residuals of a linear response function model in column 3 and the resultant uncertainties of the residuals u_{r} in column 4.

'rungs' of the ladder.

The depth of each groove is evaluated by fitting two parallel planes to topography points of regions on the reference plane in the vicinity of the groove and a region at the center of the groove bottom area as indicated in Fig. 7. The procedure is specified in the draft standard ISO 25178-700 as an areal extension close to the method of ISO 5436-1 [11]. The nominal width at the bottom is $w = 300\,\mu$m and the nominal width between neighboring grooves is $400\,\mu$m. At the sides of one groove, the reference plane areas $\{A, B\}$ have a distance of $\frac{w}{3} = 100\,\mu$m to the top edges and a width of $\frac{2w}{3} = 200\,\mu$m. The plane area C at the bottom center has a width of $100\,\mu$m. The reference plane areas $\{A_j, B_j\}$ of different grooves j may not exactly lie on the same level. This type of systematic uncertainty has been modeled as bow with its maximum being $u_{\mathrm{bow}} = 0.3\,\mu$m.

All these contributions have been included into a Monte Carlo simulation using the example of the synthetic data set shown in Fig. 5 and using the uncertainties $u(d_{\mathrm{C}})$ stated in the calibration certificate. As well, the depth uncertainty $u(d_{\mathrm{In}})$ of the example of measured data shown Fig. 6 has been chosen as a further contribution to the uncertainty budget.

The uncertainty of the certified calibration values of the different depths differ according to their height, the deepest groove of 5 mm depth has a significantly larger uncertainty of $u(d_{\mathrm{C},6}) = 0.1\,\mu$m dominating the effect of influences of $u(d_{\mathrm{C}})$. Table 1 is an example uncertainty budget.

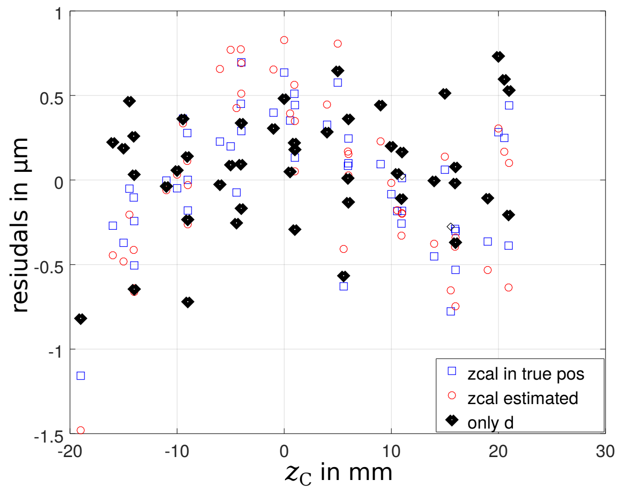

Figure 8: Uncertainty estimation by superimposing the synthetic linearity deviation Simulation of Fig. 5 with uncertainty influences $u(d_{\mathrm{C}})$,$u(d_{\mathrm{In}})$, and $u(d_{\mathrm{bow}})$ that yield a bias of the estimation of systematic linearity deviations.

The quantities of the second column display the uncertainty of the components $u(d_i) = u(d_{\mathrm{C}})$, $u(d_{\mathrm{In}})$, and $u(d_{\mathrm{bow}})$ respectively with the subscript i representing the subscripts C, In, and bow. The third column states the sensitivities by running the Monte Carlo simulation each time for only one of the three components yielding uncertainties u_{r} of the residuals of the regression line of z_{In} vs. z_{C} that are displayed in column four. The combined uncertainty u_{r} of the linearity deviation is obtained by including all three components to the Monte Carlo simulation. For the example, the combined uncertainty ranges from $u_{\mathrm{r}} = 0.2\,\mu\mathrm{m}$ to $0.4\,\mu\mathrm{m}$. This value is independent of the choice of the amplification factor. We used different curvatures, spatial wavelengths of nonlinearity of $\lambda = 30\,\mathrm{mm}$ and $70\,\mathrm{mm}$, and used different phase shifts $\Delta z = 0$ and $10\,\mathrm{mm}$. Fig. 8 illustrates the influence of random uncertainty effects of $u(d_{\mathrm{C}})$ and $u(d_{\mathrm{In}})$ together with the systematic effect of a bow $u(d_{\mathrm{bow}})$ deteriorating the determination of linearity deviations as systematic trend of the instruments axial scanning system.

6. Conclusion

It has been shown that a determination of the amplification factor and the linearity deviations is possible using a fast and simple method with little expense and effort, well suited for industrial routine calibration in the field. This method is realized by using a small set of grooves on one common depth setting artefact. If the uncertainties of the material measures and the random positioning uncertainty of the instrument are significantly smaller than the linearity deviation, an adjustment of the non-linearity is possible. Simulations show how to distinguish systematic and random influences and that a response function can be obtained for small uncertainties of the material measure and the instrument's positioning.

A new standard on *Calibration and verification of areal topography measuring instruments* is being drafted [1], ISO 25178-700, which allows a simplified calibration procedure of the amplification factor and non-linearities. If the response curve resulting from the simplified procedure shows irregularities, it is necessary to apply procedures that require more effort.

Acknowledgement

We thank Prof. Richard Leach, University of Nottingham, for his fruitful comments and thorough proof reading of the manuscript. We also thank the anonymous reviewers for providing helpful comments on earlier drafts of the manuscript. All the suggestions helped to improve and clarify the paper.

References

[1] ISO/CD 25178-700, Geometrical Product Specifications – Surface texture: Areal – Part 700: Calibration, adjustment and verification of areal topography measuring instruments, under development.

[2] W. Bauer, Special properties of coherence scanning interferometers for large measurement volumes, J. Phys.: Conf. Ser. 311 (2011) 012030. doi:10.1088/1742-6596/311/1/012030.

[3] ISO 9001:2015, Quality management systems – Requirements (2015).

[4] JCGM 200:2012, International Vocabulary of Metrology – Basic and General Concepts and Associated Terms (2012).
URL https://www.bipm.org/en/publications/guides/vim.html

[5] S. Kiyono, W. Gao, S. Zhang, T. Aramaki, Self-calibration of a scanning white light interference microscope, Optical Engineering 39 (10) (2000) 2720 – 2725. doi:10.1117/1.1290471.

[6] S. Boedecker, C. Rembe, H. Schmid, T. Hageney, T. Köhnlein, Calibration of the z-axis for large-scale scanning white-light interferometers, J. Phys.: Conf. Ser. 311 (2011) 012027. doi:10.1088/1742-6596/311/1/012027.

[7] C. L. Giusca, S. Goel, Improved and simpler estimation of scale linearity contribution to topography measurement, Precision Engineering 60 (2019) 368 – 373. doi:10.1016/j.precisioneng.2019.09.002.

[8] R. Leach, C. Giusca, H. Haitjema, C. Evans, X. Jiang, Calibration and verification of areal surface texture measuring instruments, CIRP Annals 64 (2) (2015) 797–813. doi:10.1016/j.cirp.2015.05.010.

[9] C. Giusca, R. Leach, F. Helery, Calibration of the scales of areal surface topography measuring instruments: part 2. amplification, linearity and squareness, Meas. Sci. Technol. 23 (6) (2012) 065005. doi:10.1088/0957-0233/23/6/065005.

[10] ISO 25178-600:2019, Geometrical Product Specifications – Surface texture: Areal – Part 600: Metrological characteristics for areal-topography measuring methods (2019).

[11] ISO 5436:2000, Geometrical Product Specifications (GPS) – Surface texture: Profile method; Measurement Standards – Part 1: Material Measures (2000).